

# Resonance Raman Optical Activity and Surface Enhanced Resonance Raman Optical Activity Analysis of Cytochrome *c*

Christian Johannessen,<sup>†</sup> Peter C. White,<sup>‡</sup> and Salim Abdali\*<sup>\*,†</sup>

Quantum Protein Centre, QuP, Department of Physics, Technical University of Denmark, DK-2800 Kgs. Lyngby, Denmark, and Department of Forensic and Biomedical Sciences, University of Lincoln, Brayford Pool, Lincoln LN6 7TS, U.K.

Received: January 22, 2007; In Final Form: March 16, 2007

High-resolution resonance Raman (RR) and resonance Raman optical activity (ROA) spectra of cytochrome *c* were obtained in order to perform full assignment of spectral features of the resonance ROA spectrum. The resonance ROA spectrum of cytochrome *c* revealed a distinct spectral signature pattern due to resonance enhanced skeletal porphyrin vibrations, more pronounced than any contribution from the protein backbone. Combining the intrinsic resonance properties of cytochrome *c* with the surface plasmon enhancement achieved with colloidal silver particles, the surface enhanced resonance Raman scattering (SERRS) and surface enhanced resonance ROA (SERROA) spectra of the protein were successfully obtained at concentrations as low as 1  $\mu$ M. The assignments of spectral features were based on the information obtained from the RR and resonance ROA spectra. Excellent agreement between RR and SERRS spectra is reported, while some disparities were observed between the resonance ROA and SERROA spectra. These differences can be ascribed to perturbations of the physical properties of the protein upon adhesion to the surface of the silver colloids.

## 1. Introduction

Spectroscopic analysis of biomacromolecules in solution has become an important accessory in the full structural characterization of biomacromolecules and is typically performed by crystallization and X-ray diffraction techniques. Optical spectroscopic techniques such as vibrational absorption spectroscopy, e.g., Raman scattering, are powerful tools for studying biomolecules in solution. However, these techniques provide less structural information than X-ray diffraction, restricting the analysis to determination of local structure elements,<sup>1,2</sup> unless combined with structural computation such as *ab initio* calculations.<sup>3,4</sup> On the other hand, vibrational optical spectroscopy of biomacromolecules in solution allows analyses of molecular dynamics, since the biomacromolecules are closer to or in their native environments instead of being in the crystal phase.<sup>5,6</sup> Unfortunately, high sample concentrations are usually required for useful spectroscopic measurements, limiting the analysis to highly soluble compounds.

One of the strategies that has been successfully used in the analysis of dilute samples of biomacromolecules is surface enhanced Raman scattering (SERS).<sup>7–9</sup> Originally, SERS was observed as a fortunate side effect when molecules were adsorbed on roughened metal electrodes, but it has now developed into a versatile tool for chemical analysis in that SERS allows enhancement of Raman scattering cross sections up to  $10^{14}$ , which has enabled spectroscopic measurements to be obtained at the single molecule level.<sup>8–10</sup> This enhancement of Raman active transitions occurs due to a coupling of the electronic transitions in the sample molecule and the surface plasmon resonances in the metal colloidal particles, to which the sample molecules are adsorbed.<sup>8</sup> Therefore, the enhancement

depends on the laser excitation of the surface plasmon resonance, which again is dependent on the metal (usually Ag or Au) and the average size of the particles. Developing stable colloidal suspensions of metallic nanoparticles of a uniform size has now allowed SERS to be performed in solution, and not solely on a metal surface.<sup>9</sup>

To take full advantage of the surface plasmon resonance enhancement observed in SERS, an obvious next step was to combine this effect with another structurally sensitive spectroscopic method, i.e., Raman optical activity (ROA). Recently, using this combination we were able to apply surface plasmon resonance enhancement in ROA measurements of the pentapeptide enkephalin<sup>11</sup> and the oxygen storage molecule myoglobin.<sup>12</sup> As ROA measures the difference in scattering of circularly polarized light by optically active molecules, the method is extremely sensitive to structural components in biomacromolecules, most of which are chiral.<sup>13</sup> While ROA certainly has proved to be an invaluable tool in biomolecular research, the method is hampered by the need for high sample concentrations and long measuring times, hence limiting industrial applications. By enhancing the ROA signals from the molecules in question, we were able to significantly reduce the acquisition time of the measurements, and more importantly reduce the concentration of the sample considerably, thus allowing structural information to be obtained from very dilute samples. This novel approach has been called surface enhanced ROA (SEROA), and the first reliable results were published earlier.<sup>11</sup>

In our previous study of myoglobin, the advantage of an additional enhancement effect in Raman spectroscopy, namely resonance Raman (RR),<sup>12</sup> was achieved. Resonance enhancement of Raman scattering occurs when an electronic transition is triggered by the excitation laser. The electronic excitation increases the Raman scattering probability of vibrational normal modes in the spatial vicinity of the chromophore, hence enhancing these signals in the resulting spectrum.<sup>14</sup> The RR

\* Corresponding author. E-mail: abdali@fysik.dtu.dk.

<sup>†</sup> Technical University of Denmark.

<sup>‡</sup> University of Lincoln.

enhancement couples with surface plasmon enhancement, resulting in a very strong enhancement of certain signals, known as surface enhanced resonance Raman scattering (SERRS).<sup>15,16</sup> SERRS measurements are of course only possible when there is frequency overlap between the electronic transition of the sample and the surface plasmon resonance of the nanoparticles in question.

RR has been extensively exploited in the analysis of difficult (e.g., chromophoric) biological samples. This again allows for reduction of sample concentration; however, little effort has been devoted to development of the resonance ROA effect. This is mainly because chromophore excitation also causes fluorescence, which results in a high background signal and reduction of signal-to-noise ratio, thus making ROA measurements difficult.

As reported previously,<sup>12</sup> resonance ROA measurements were possible on chromophoric metalloproteins, such as myoglobin, but only when the sample was extensively pretreated and only by a very long measurement. SEROA measurements of myoglobin gave similar results; however, these were achieved at much lower concentrations and in shorter measuring times.<sup>12</sup>

Here, we present a full assignment of resonance ROA and SEROA signals for another globular metalloprotein, cytochrome *c*. The assignment of spectral features in the high resolution resonance ROA spectrum of cytochrome *c* reveals a distinct ROA signature pattern for porphyrin, clearly distinguishable from the patterns normally observed for the protein backbone. By combining surface plasmon enhancement of silver nanoparticles with Q-band excitation of the heme, this paper shows that it is possible to measure and assign the SERRS and SERROA spectra of cytochrome *c* by direct comparison with the RR and resonance ROA spectra. While several spectral features were conserved in the SERROA spectrum, some spectral differences reveal the perturbation of the physical properties of cytochrome *c* when using surface plasmon enhancement.

## 2. Materials and Methods

**2.1. Preparation of Colloids and Samples.** Silver colloids were produced by hydroxylamine hydrochloride reduction based on the method originally developed by Leopold and Lendl.<sup>17</sup> All glassware was soaked in aqua regia (HNO<sub>3</sub>/HCl 1:3 v/v) for 24 h, followed by gentle rubbing with a soap solution, and finally rinsing with Milli Q water. A stock solution of 0.33 M sodium hydroxide (1.332 g in 100 mL of Milli Q water) was prepared, and 1 mL of this solution was transferred to a 100 mL volumetric flask and diluted to the mark with Milli Q water. A volume of this solution (90 mL) was placed in a single-neck round-bottom flask (250 mL) and stirred with a magnetic stirrer at room temperature. Hydroxylamine hydrochloride (10.4 mg) was added to the flask, and after stirring for 5 min silver nitrate (10 mL of a 10<sup>-2</sup> M solution; 34 mg/20 mL of Milli Q water) was added in one aliquot. The solution was stirred for a further 15 min, and then the colloid was stored in a sealed container and in the dark at room temperature until required.

Horse heart cytochrome *c* (purity >95%), purchased from Sigma, was used without further purification. The sample was dissolved in Milli Q water to a stock solution of 100 μM and kept at 4 °C until use. For the resonance ROA measurements, the sample was pretreated by filtering through a 22 μm Millipore filter and centrifuged for 10 min at 4000 rpm. The sample was then exposed to laser light (532 nm, 500 mW at sample) in order to quench fluorescence caused by trace impurities. For the SEROA measurements, the stock solution was filtered again,

followed by dilution with Milli Q water and mixed with Ag colloid and NaCl solutions to give a final protein concentration of 1 μM. The concentration of Ag colloid was determined by the optimization procedure (described in refs 12 and 18) and required 90% (v/v) Ag colloid, 10% (v/v) cytochrome *c*, and 10 μL of 0.5 M NaCl to give a final concentration of 0.025 M NaCl in 200 μL of the sample solution. After the components were mixed, the samples were left for 15 min before measuring.

**2.2. Spectroscopic Analysis.** All measurements were carried out on a ChiralRAMAN scattered circular polarization spectrometer (BioTools Inc., USA). This instrument simultaneously provides Raman and ROA spectra and is equipped with a 532 nm laser source (Excel, Laser Quantum, U.K.) and a back thinned CCD detector, optimized for recording in the spectral range 100–2400 cm<sup>-1</sup>. The spectral resolution, limited by the width of the individual optical fiber at the entrance of the spectrograph, is 7 cm<sup>-1</sup>. The ROA spectra are presented as circular polarization intensity differences ( $I_R - I_L$ ), where  $I_R$  and  $I_L$  denote the intensities of the right and left circularly polarized components of the scattered light, respectively. The parent Raman spectra are presented as corresponding circular polarization intensity sums ( $I_R + I_L$ ).

Resonance ROA spectra of cytochrome *c* were obtained with a laser power of ~500 mW at the sample and acquisition times of 16–20 h, while the SERROA spectra were obtained with a laser power of ~70 mW at the sample and a 30 min acquisition time.

In order to verify the SERROA measurements, control samples were prepared by replacing either protein or colloids with Milli Q water. These control samples were analyzed to rule out any contribution to the SERROA spectra of cytochrome *c* from either the colloid or the non surface enhanced resonance ROA signals produced by cytochrome *c*.

## 3. Results and Discussion

**3.1. Assignment of the Resonance ROA Spectrum of Cytochrome *c*.** The RR spectrum of cytochrome *c* has been previously analyzed in detail, and all significant peaks have been assigned.<sup>19–21</sup> As the resonance enhancement originates from electronic transitions in the iron–porphyrin complex, all Raman signals can be assigned to porphyrin vibrations, effectively concealing any contributions from the protein, except for stretching vibrations of the carbon–sulfur bonds that covalently link porphyrin to two cysteine residues in the protein backbone. Comparing the RR spectrum (Figure 1a) with the comprehensive analysis of cytochrome *c* RR spectral data published by Hu and co-workers,<sup>21</sup> it was possible to determine the origin of all major contributions to the spectrum (see Table 1). The corresponding resonance ROA spectrum of cytochrome *c* (Figure 1b) exhibits distinct chiral signals that all appear in good agreement with RR peaks. In addition to the obvious overlap between signals in the RR and resonance ROA spectra of cytochrome *c*, the resonance ROA observed in Figure 1b does not resemble an ordinary ROA spectrum of a globular protein,<sup>5</sup> allowing the assumption that the chiral signals are indeed due to vibrations of the porphyrin ring.

In the 1700–1100 cm<sup>-1</sup> range, most RR signals are assigned to strongly enhanced in-plane vibrations that also give rise to contributions from the major resonance ROA (see Figure 1). While the  $\nu_{10}$  and  $\nu_{11}$  transitions have positive resonance ROA, the  $\nu_{19}$  signal, located between these vibrations, appears to be a negative–positive couplet, indicating contributions from two transitions. A strong positive or negative bias in ROA spectra is usually an indication of spurious signals, but we believe that

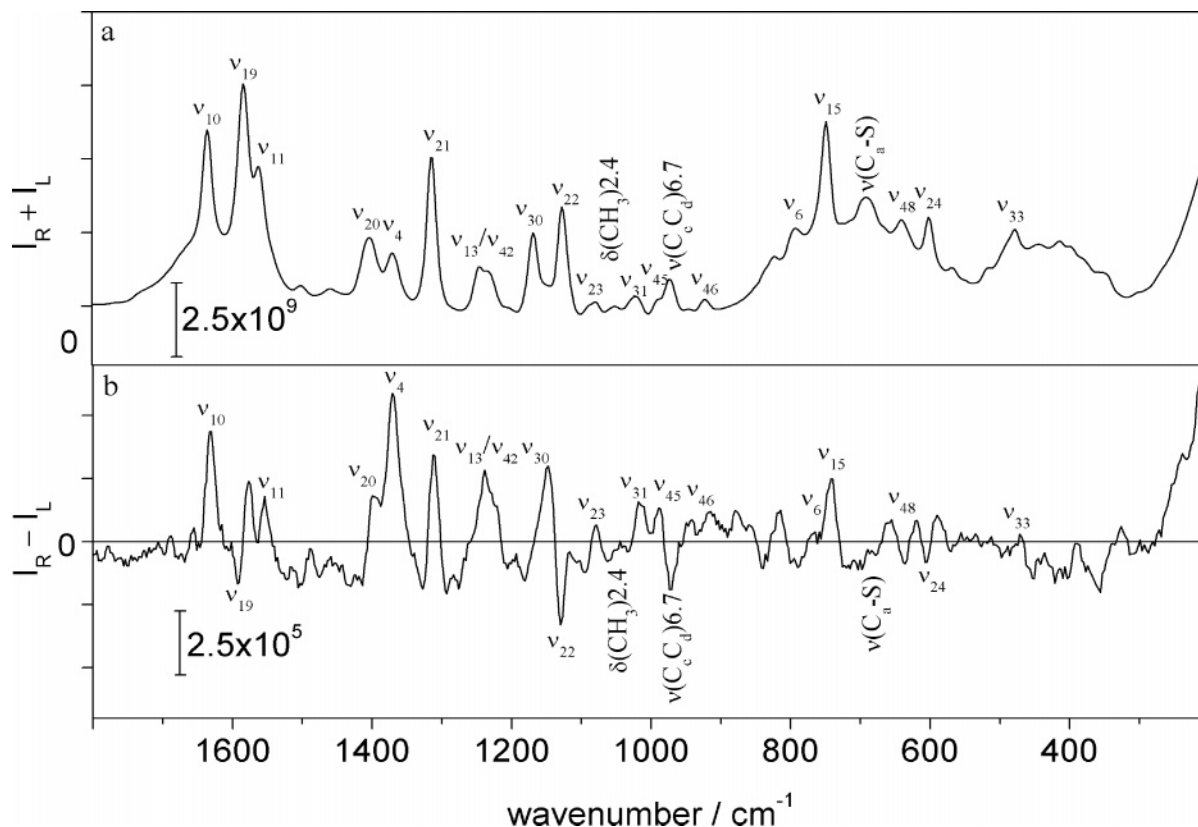


**Figure 1.** Resonance Raman (a) and resonance ROA (b) spectra of cytochrome *c* in aqueous solution (100  $\mu\text{M}$ ). The spectra were obtained simultaneously as described in the text. For assignment details, see Table 1.

**TABLE 1: Resonance Raman and Surface Enhanced Resonance Raman Frequencies of Cytochrome *c* with Normal Mode Assignment and Allocation of Local Coordinates**

RR <sup>a</sup>	SERRS <sup>b</sup>	literature <sup>c</sup>	assignment <sup>c</sup>	local coordinates <sup>d</sup>
1635	1635	1626/1636	$\nu_{10}$	$\nu(\text{C}_\alpha\text{C}_m)_{\text{asym}}$
1584	1582	1587	$\nu_{19}$	$\nu(\text{C}_\alpha\text{C}_m)_{\text{asym}}$
1561	1562	1551	$\nu_{11}$	$\nu(\text{C}_\beta\text{C}_\beta)$
1402	1402	1400	$\nu_{20}$	$\nu(\text{pyr quarter ring})$
1371	1371	1364	$\nu_4$	$\nu(\text{pyr half ring})_{\text{sym}}$
1315	1316	1314	$\nu_{21}$	$\delta(\text{C}_m\text{H})$
1246	1243	1232 (1211)	$\nu_{13}$ ( $\nu_{42}$ )	$\delta(\text{C}_m\text{H})$
1168	1169	1174	$\nu_{30}$	$\nu(\text{pyr half ring})_{\text{sym}}$
1127	1127	1130	$\nu_{22}$	$\nu(\text{pyr half ring})_{\text{sym}}$
1078	1085	1080	$\nu_{23}$	$\nu(\text{C}_\beta\text{C}_1)_{\text{asym}}$
1052	1052	1050		$\delta(\text{CH}_3)_{2,4}$
1021	1021	1032	$\nu_{31}$	$\nu(\text{C}_\beta\text{C}_1)_{\text{asym}}$
989	989	990	$\nu_{45}$	$\nu(\text{C}_\beta\text{C}_1)_{\text{asym}}$
974	974	975		$\nu(\text{C}_c\text{C}_d)_{6,7}$
923	923	925	$\nu_{46}$	$\delta(\text{pyr deform})_{\text{asym}}$
792	789	796	$\nu_6$	$\nu(\text{pyr breathing})$
748	747	750	$\nu_{15}$	$\nu(\text{pyr breathing})$
690	689	692		$\nu(\text{C}_a\text{-S})$
639	638	633/642	$\nu_{48}$	$\delta(\text{pyr deform})_{\text{sym}}$
602	597	603	$\nu_{24}$	$\delta(\text{pyr deform})_{\text{asym}}$
477	470	479	$\nu_{33}$	$\delta(\text{pyr rotat})$

<sup>a</sup> RR, resonance Raman presented here (Figure 1a). <sup>b</sup> SERRS, surface enhanced resonance Raman scattering presented here (Figure 2a). <sup>c</sup> Reference 21. <sup>d</sup> For the definition of local coordinates of porphyrin vibrations, see refs 22 and 23.

the spectrum presented is genuine. A comparison of the resonance ROA spectra of cytochrome *c* and myoglobin strongly suggests that the observed signals are of porphyrin in a chiral environment.<sup>12</sup>

The next contributions from the in-plane transitions can be assigned to  $\nu_{20}$  and  $\nu_4$ , which are enhanced (due to resonance) differently in RRS and RROA (comparing Figure 1a and 1b).

In RRS, this transition is highly dependent on the excitation wavelength, and accordingly, its intensity is hardly enhanced when 532 nm is used, while in RROA the enhancement of especially  $\nu_4$  is very obvious. This may be ascribed to the collective half-ring stretching vibration responsible for the  $\nu_4$  signal being highly chiral, resulting in a strong signal, as observed in Figure 1b. Negative resonance ROA signals in this region are found between RRS peaks, hence making assignment difficult. A possible explanation is that they are most likely due to the reverse symmetry in-plane transitions coupled to the signals of the region. While the  $\nu_{21}$  vibration gives a positive contribution to the resonance ROA spectrum, the overlapping of  $\nu_{13}$  and  $\nu_{42}$  peaks produces a slightly noisy ROA contribution. The well-resolved  $\nu_{30}$  and  $\nu_{22}$  signals give rise to a strong positive–negative couplet, allowing for unambiguous assignment of a negative ROA contribution in the high wavenumber region.

Between 1100 and 800  $\text{cm}^{-1}$  a number of less-enhanced signals can be assigned to local in-plane vibrations, deformations, and side chain vibrations with correspondingly weak ROA contributions. A noticeable exception is the two overlapping bands assigned to  $\nu_{45}$  and the propionate stretching vibration at 974  $\text{cm}^{-1}$ , which can be seen as a positive–negative couplet in the resonance ROA spectrum. The strongly enhanced  $\nu_{15}$  is the main feature of the wavenumber region below 800  $\text{cm}^{-1}$ , again giving rise to a positive resonance ROA signal, whereas the remaining signals in the region exhibit limited or no ROA.

**3.2. Assignment of SERRS and SERROA Spectra of Cytochrome *c*.** The SERRS spectrum obtained for this analysis (see Figure 2a) is remarkably similar to the RR spectrum presented in Figure 1a, and a full assignment of the relevant peaks can be seen in Table 1.

Other than a slight fluorescence background in the SERRS spectrum, the main differences between the RR and SERRS

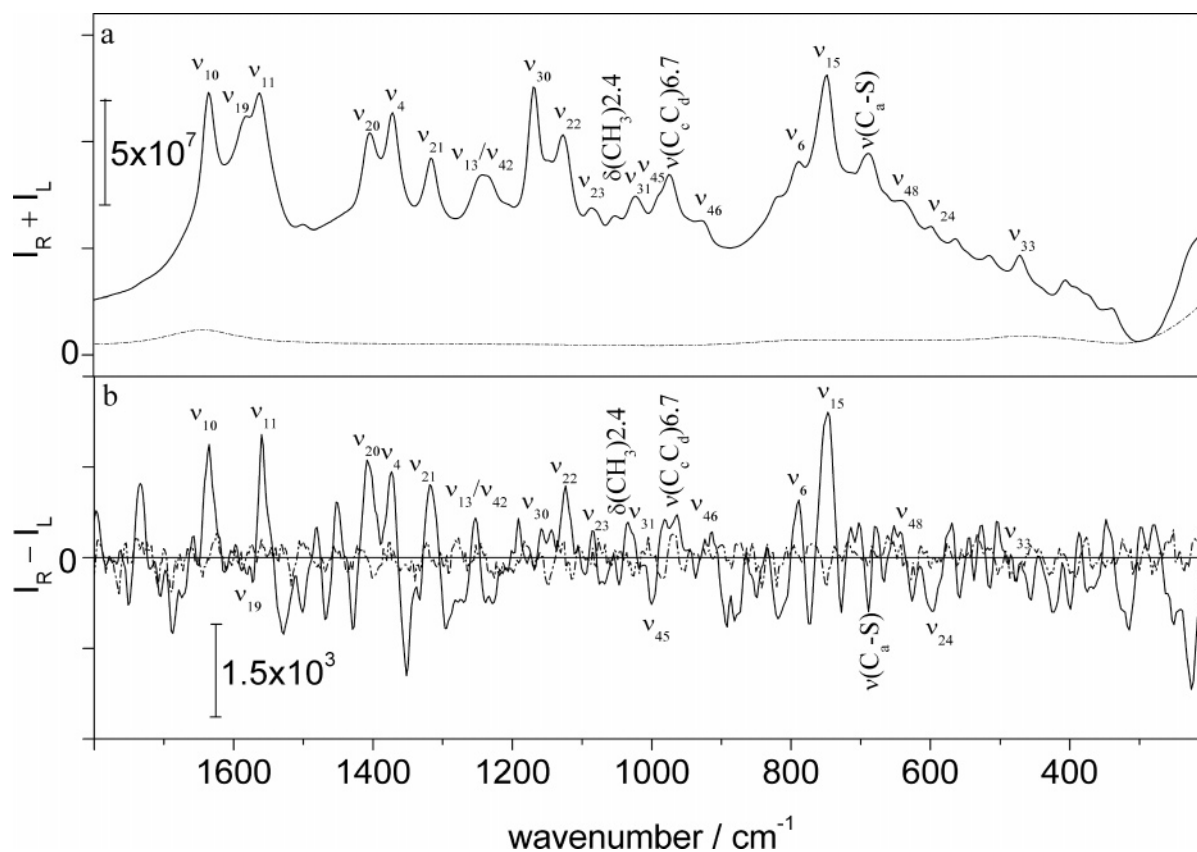


**Figure 2.** SERRS (a) and SERROA (b) spectra of cytochrome *c* in aqueous/colloidal solution (1  $\mu$ M protein). Control spectra of colloid and water mixtures are included in both figures (dotted lines). Spectra were obtained as described in the text. For assignment details, see Table 1.

spectra are the following: the selective surface plasmon enhancement of transitions  $\nu_{10}$  and  $\nu_{11}$ , almost concealing  $\nu_{19}$ ; the stronger enhancement and inversion of intensity relation of  $\nu_{20}$  and  $\nu_4$  compared to  $\nu_{21}$ ; and the inversion of intensity relation of  $\nu_{30}$  and  $\nu_{22}$ . In Figure 2a, the spectrum of a negative control sample, prepared by replacing protein with water, is also presented (dotted line), and in this spectrum, no signals are seen (except for the water band at approximately  $1625\text{ cm}^{-1}$ ), a matter that verifies the authenticity of the SERRS cytochrome *c* signals seen in Figure 2a (solid line). Similar results were observed when recording spectra of protein samples of  $1\ \mu\text{M}$  concentration without colloid (not shown here).

The SERROA spectrum of cytochrome *c*, presented in Figure 2b (solid line), retains several of the main features of the resonance ROA spectrum presented in Figure 1b. In analogy with the SERRS spectrum (Figure 2a), Figure 2b also includes a negative control spectrum (dotted line) of a mixture of colloids and water, which produces no signals but shows the noise level of the measurement in a colloidal suspension.

It is worth noticing that there is some degree of correlation between the enhancements of Raman active transitions in SERRS (Figure 2a) and the corresponding SERROA signals. In the wavenumber region above  $1100\text{ cm}^{-1}$ , the peaks corresponding to the  $\nu_{10}$  and  $\nu_{11}$  transitions reproduce the positive signals seen in the resonance ROA spectrum (see Figure 1b), while the  $\nu_{19}$  couplet is decreased to the noise level. In addition to the fact that this transition appears to be less enhanced by the plasmon effect compared to the two other transitions, the lack of a SERROA signal can also be due to an increased polarization of the transition (or transitions), resulting in artifact prone data collection. This effect is often seen in ROA spectra,<sup>24</sup> and it would be natural to assume that several

transitions of a molecule adsorbed on a metal surface would exhibit strong polarization.

In this range ( $>1100\text{ cm}^{-1}$ ), a SERROA signal at  $1732\text{ cm}^{-1}$  was observed and this was not present in the corresponding SERRS spectrum, a result not previously observed. This signal cannot readily be assigned to a protein transition, unless the frequency of such a vibration is heavily shifted, nor to any of the small molecules (primarily  $\text{NH}_4^+$ ) produced as byproducts in preparation of the colloids. This feature does demonstrate the sensitivity of the SERROA, even to vibrations that are not detectable with SERS. The  $\nu_{20}$  SERROA signal is in good agreement with the resonance ROA, whereas the  $\nu_4$  SERROA signal is considerably less enhanced in comparison to other peaks in this region (see Figure 2b). This feature is rather interesting, as the SERRS spectrum of cytochrome *c* shows a favorable enhancement of the  $\nu_4$  transition compared to  $\nu_{20}$ , while the resonance ROA of  $\nu_4$  is very pronounced (see Figure 1b), an effect that is apparently reversed in the SERROA spectrum.

Considering this region, it is worth noticing that, while the signals observed in the resonance ROA (Figure 1b) tend to be biased positively, they appear more balanced (positive–negative intensity) in the SERROA spectrum (Figure 2b); most significant is the strong negative band below the positive signal assigned to  $\nu_4$ . This leads us to believe that  $\nu_4$  in fact can be assigned to a positive–negative couplet, strongly polarized in the resonance ROA measurement. Countering the polarization of this transition could be due to a change in the dipole moment, when the molecule adsorbs to the silver colloids, yielding more intensity of the negative signal in the couplet. The SERROA signal assigned to  $\nu_{21}$  appears very similar to the resonance ROA signal when compared to the surrounding bands (see Figure 2b), while

the corresponding SERRS signal is weak compared to the RR spectrum (see Figure 1a). Recently, Janesko and Scuseria formulated theoretical tools for analyzing the electromagnetic effect in surface enhancement of ROA.<sup>25</sup> The theoretical derivation of the electromagnetic effect indicates, among other things, that quadrupolar responses of the substrate (here the silver) may significantly enhance ROA in certain cases, which could explain the apparent lack of SERRS signal from  $\nu_{21}$ , as the SERROA signal is favorably enhanced.

In the resonance ROA spectrum of cytochrome *c* (Figure 1b), the features originating from the close-lying  $\nu_{13}$  and  $\nu_{42}$  bands were assigned to one broad positive contribution (see Table 1). While the SERRS signals from these two transitions appear similar, the SERROA spectrum exhibits only one feature, a narrow positive signal located at  $1243\text{ cm}^{-1}$ . We believe that the poorly resolved resonance ROA signals are possibly due to polarization of the transitions<sup>26</sup> and that this feature is carried over in the SERROA spectrum, resulting in a spurious signal.

In contrast to these two transitions, the resonance ROA contributions from  $\nu_{30}$  and  $\nu_{22}$  are very well resolved (see Figure 1b). As mentioned above, the SERRS spectrum shows an inverse intensity relation of these two bands. In the SERROA spectrum of cytochrome *c*, the  $\nu_{30}$  band is decreased to the noise level, while the  $\nu_{22}$  band is positive, resulting in the absence of the well-resolved couplet observed in the resonance ROA spectrum. This rather profound change can be explained by changes in the dipole moment and polarization of the molecule when adhering to the silver colloids as indicated previously. However, it may also arise from symmetry changes in the porphyrin. Both transitions are symmetric in-plane half-ring stretching vibrations, and while the negation of the  $\nu_{30}$  contribution seems to be an unfortunate coincidence, the full inversion of the  $\nu_{22}$  band indicates a possible symmetry inversion in the prosthetic group. This change is even more pronounced when examining the weak couplet, assigned to  $\nu_{45}$  overlapping the propionate stretching vibration at  $974\text{ cm}^{-1}$  in the resonance ROA spectrum. While this couplet was positive–negative in this spectrum (see Figure 1b), the SERROA spectrum reveals a weak negative–positive couplet, with the negative portion of the couplet commencing immediately after  $\nu_{31}$ . In addition to being an interesting contribution to the overall understanding of plasmon effect and the influence on adsorbed molecules to metal surfaces, the inversion of these bands also shows how cautious one must be when using ROA spectra to assign spectral features in SERROA spectra.

The low wavenumber region ( $<1100\text{ cm}^{-1}$ ) of the SERROA spectrum is dominated by two strong signals (at  $789$  and  $747\text{ cm}^{-1}$ ), while the rest of the features visible in the SERRS spectrum appear to be nearly lost in the noise level of the SERROA spectrum. The two features, both positive, can be assigned to the  $\nu_6$  transition and the strongly resonance enhanced  $\nu_{15}$  transition. The  $\nu_6$  was not discussed in the assignment of the resonance ROA spectrum, as this region of the spectrum is rather noisy, but a tentative assignment could be made to the broad negative feature next to the  $\nu_{15}$  band. If this is the case, the  $\nu_6$  band is again inverted compared to that in SERRS. The  $\nu_{15}$  band is strongly positive in the SERROA spectrum compared to the rest of the spectral features, but does not change sign. Again, this shows the complexity of changes induced in the protein when adsorbing to the surface of the silver colloids. Both  $\nu_6$  and  $\nu_{15}$  are breathing modes of the porphyrin ring, and a symmetry inversion should affect both modes equally, so changes in the dipole moment and polarization must also contribute to the final spectral features.

Accordingly, the assignment of cytochrome *c* resonance ROA and subsequently SEROA spectra proved to be possible and to reveal useful information about the physical changes induced in the molecule analyzed by surface plasmon enhanced Raman spectroscopy, as well as new information about the compound itself. One feature of the SERROA spectrum that could cause some concern is the high noise level that could be problematic when analyzing samples with low-intensity bands. Here it must be stressed that the enhancement effect in itself must be strong enough to counter such noise, and that samples exhibiting no explicit SERROA signals should not be considered. It is also worth mentioning in this context that the SERROA spectrum was measured extremely rapidly at 100 times lower concentration, 8 times less laser power, and 40 times less total acquisition than for the corresponding resonance ROA spectrum. In order to verify the SERROA technique, a benchmark investigation would be desirable, in which an enantiomeric pair of molecules provides mirror-imaged ROA and SEROA. This investigation would prove, beyond doubt, whether genuine SEROA measurements can be obtained from one enantiomer. However, the protocol presented here is optimized for proteins, and naturally restricts measurements to one enantiomer.

#### 4. Conclusion

Resonance Raman (RR) and resonance Raman optical activity (ROA) measurements on cytochrome *c* in solution led to the assignment of spectral features in the resonance ROA spectrum of the compound, revealing a distinct spectral pattern for the resonance enhanced porphyrin vibrations observed in the spectrum. Based on these results, spectra of cytochrome *c* obtained by surface enhanced resonance Raman scattering (SERRS) and surface enhanced resonance ROA (SERROA) were assigned. While the SERRS spectrum had a remarkable resemblance to the RR spectrum, the resonance ROA and SEROA spectra exhibited both similar and quite different signal patterns, believed to be due to changes in the physical properties measured in the optical activity spectrum. Taking spectral changes into account, a full assignment of the SERROA spectrum of cytochrome *c* was possible, based on a measurement performed on a highly diluted sample ( $1\text{ }\mu\text{M}$ ) and at short measuring time (30 min). In general, using SEROA in biophysical research could reveal much needed insight into the physical mechanisms resulting in surface plasmon enhancement, and the method could prove invaluable in the future, e.g., in analyzing dilute protein samples in laboratories and clinics.

**Acknowledgment.** Prof. L. D. Barron and Dr. L. Hecht are acknowledged for fruitful discussions during and after a visit to Glasgow University by one of the authors (C.J.). This work was supported by the Danish Fundamental Research Foundation (2001–2009).

#### References and Notes

- (1) Kiederling, T. A. *Curr. Opin. Chem. Biol.* **2002**, *6*, 682.
- (2) Nafie, L. A. *Annu. Rev. Phys. Chem.* **1997**, *48*, 357.
- (3) Abdali, S.; Jalkanen, K. J.; Cao, X.; Nafie, L. A.; Bohr, H. *Phys. Chem. Chem. Phys.* **2004**, *6*, 2434.
- (4) Johannessen, C.; Thulstrup, P. W. accepted by *Dalton Trans.* **2007**, in press; DOI:10.1039/b618995d.
- (5) Barron, L. D.; Hecht, L.; Blanch, E. W.; Bell, A. F. *Prog. Biophys. Mol. Biol.* **2000**, *73*, 1.
- (6) Nibbering, E. T. J.; Fidler, H.; Pines, E. *Annu. Rev. Phys. Chem.* **2005**, *56*, 337.
- (7) Fleishmann, M.; Hendra, P. J.; McQuillan, A. J. *Chem. Phys. Lett.* **1974**, *24*, 163.
- (8) Kerker, M. *Pure Appl. Chem.* **1981**, *53*, 2083.
- (9) Moskovits, M. *J. Raman Spectrosc.* **2005**, *36*, 485.

- (10) Aroca, R. *Can. J. Anal. Sci. Spectrosc.* **2004**, *49*, 114.  
(11) Abdali, S. *J. Raman Spectrosc.* **2006**, *37*, 1341.  
(12) Abdali, S.; Johannessen, C.; Nygaard, J.; Norbygaard, Th. *J. Phys.: Condens. Matter* **2007**, *19*, 285205.  
(13) Barron, L. D.; Hecht, L.; McColl, I. H.; Blanch, E. W. *Mol. Phys.* **2004**, *102*, 731.  
(14) Bobovich, Y. S.; Bortkevich, A. V. *Sov. J. Quantum Electron.* **1977**, *7*, 269.  
(15) Jeanmaire, D. L.; Van Duyne, R. P. *J. Electroanal.* **1977**, *84*, 1.  
(16) Cotton, T. M.; Schultz, S. G.; Van Duyne, R. P. *J. Am. Chem. Soc.* **1980**, *102*, 7962.  
(17) Leopold, N.; Lendl, B. *J. Phys. Chem. B* **2003**, *107*, 5723.  
(18) Nygaard, J. Determination of Myoglobin by Raman and SERS Spectroscopy. M.Sc. Thesis, Quantum Protein Centre, QuP, Department of Physics, Technical University of Denmark, 2006.  
(19) Strekas, T. C.; Spiro, T. G. *Biochim. Biophys. Acta* **1972**, *278*, 188.  
(20) Spiro, T. G.; Strekas, T. C. *Proc. Natl. Acad. Sci. U.S.A.* **1972**, *69*, 2622.  
(21) Hu, S.; Morris, I. K.; Singh, J. P.; Smith, K. M.; Spiro, T. G. *J. Am. Chem. Soc.* **1993**, *115*, 12446.  
(22) Li, X.-Y.; Czernuszewicz, R. S.; Kincaid, J. R.; Su, O. Y.; Spiro, T. G. *J. Phys. Chem.* **1990**, *94*, 31.  
(23) Li, X.-Y.; Czernuszewicz, R. S.; Kincaid, J. R.; Stein, P.; Spiro, T. G. *J. Phys. Chem.* **1990**, *94*, 47.  
(24) Che, D.; Nafie, L. A. *Appl. Spectrosc.* **1993**, *47*, 544.  
(25) Janesko, B. G.; Scuseria, G. E. *J. Chem. Phys.* **2006**, *125*, 124704.  
(26) Etchegoin, P. G.; Galloway, C.; Le Ru, E. C. *Phys. Chem. Chem. Phys.* **2006**, *8*, 2624.